



The combined effects of radiation and chemical reactions influence heat and mass transfer in a mixed convective flow of micropolar fluid

*¹B. Saidulu ,²K. Sreeram Reddy and ³M. Sathyanarayana

^{1,2,3} Department of Mathematics, University College of Science, Osmania University, Hyderabad-500007, Telangana, India

Email: ¹bandhamssaidulu@gmail.com, ²dr_sreeram_reddy@yahoo.com,
³manthrisathyam926@gmail.com

* Corresponding author Email address: bandhamssaidulu@gmail.com

Abstract:

Our research aims to find a way to address the issue of heat and mass transfer in a steady mixed convection flow of an incompressible micropolar fluid over a stretched surface under influence based on thermal radiation and chemical reaction. By using MATLAB inbuilt bvp4c approach, It has been examined how important variables affect the velocities, microrotations, temperatures, and concentration functions. The numerous technical characteristics of a flow significantly affect the Sherwood numbers, Nusselt, skin-friction coefficient, and other non-dimensional distributions. According to measurements of the magnetic field, the micropolar variable must have an adverse effect on all functions except for temperature, while the micro rotational component causes objects to move more slowly but increases both temperature and concentration. With higher numbers of the Schmidt number, the temperature goes up and the concentration declines as the radiation factor increases.

Keywords: radiation, heat transfer, bvp4c, matlab.

DOI NUMBER: 10.48047/NQ.2022.20.19.NQ99432

NEUROQUANTOLOGY 2022; 20(19): 4690-4708

4690

Nomenclature

u, v	x, y – Components of velocity	j	microinertia per unit mass (N/kg)
μ	Dynamic viscosity ($kg\ m/s$)	c_p	specific heat at constant pressure ($J/Kg\ K$)
ρ	Density of the fluid (kg/m^3)	C	concentration of the fluid inside the boundary layer
ζ	similarity variable	C_w	concentration of the fluid at the surface
γ	spin gradient viscosity	M	Magnetic parameter
ν	kinematic viscosity (m^2/s)	Pr	Prandtl number
g	Gravitational acceleration	Kr	Chemical reaction parameter
u_w	surface velocity (m/s)	Sc	Schmidt number
b	constant	K	material parameter
k_f	thermal conductivity	S	surface condition parameter
D	Mass diffusion coefficient of the fluid (m^2/s)	T	Temperature across the thermal boundary layer (k)
Ec		θ	Dimensionless temperature



1. Introduction

Combined conduction of heat seems to be the term used to describe a convection thermal transfer phenomenon that takes into account either organic or artificial convection. These effects both controlled and spontaneous convection upon heat transfer during combined affected convection heat fluxes were similar in size. Convection of heat occurs frequently in natural factories, including those with cutting-edge technology, like in essential weapons without any liquid leaks, in the refrigeration of electrical parts, etc. J. Peddieson and Mcnitt [1] have studied the flow of a micropolar fluid through the boundary layer of a semi-infinite plate. So even though G. Ahmadi [2] investigated possible approximate solutions as such flow through the boundary layer of micropolar fluids through a semi-infinite surface while accounting for the impacts near microinertia along with angular velocity direction perpendicular to an x-y plane. Y.J. Kim [3] investigated the movement of polarised liquids inside an unstable magneto hydrodynamic convective field via a porous layer that was flowing vertically inside a permeable material. Ghonaim [4] investigated the experimental effects of heat conduction containing a micropolar via a plastic structure. Berker [5] investigated the movement of a dense, unsteady flow among two identical plates moving noncoaxially while maintaining a rotational acceleration. Coirier [6] examined a circulation caused by a moving noncoaxially with a little variable rotational acceleration but a liquid near infinite. Further research was done by Jena and Mathur [7] on the unidirectional convection flow that is free of thermomicropolar vapours through a naturally convective flat vertical plate. Pavlov [8] looked into the movement like an electrical conductor fluid's porous medium caused by stretching a planar, flexible sheet with the existence of a constant longitudinal magnetic field.

According to D. Lee and A. C. Eringen [9] research with liquids, the concept of micropolarity is anticipated to give a theoretical explanation for the non-Newtonian behaviour seen in some fluids. Since Soret and Dufour observed temperature diffusion, including transmission dynamics combined with induced free convection, Kafoussias and Williams [10] looked at the free surface. Currently utilising continuous transient stability, Gaikwad et al. [11] examined that start by double diffusional convective inside a multiple combination for a strain liquid film containing Stagnation-Point, along with Dufour influences. Utilising the Modified Model Permeation Estimation, Hossain and Takhar [12] also examined the impact of radioactivity mostly at free along with forceful mixed convection of a visually high-density porous medium liquid prior to a heat source flat channel for a homogeneous mass flow rate acceleration but also heat transfer. This analysis yields nonsimilar options. Ramamoorthy [13] performed a computerised analysis of a stream across the boundary surface, consequently finally transmitting magnetohydrodynamic movement of a viscous insoluble through a moderately horizontal plate under the influence, showing a consistent magnetic field concurrent with the plate but also discovering that gravitational flux thickens both kinetic energy and temperature profile layers. In order to account for overall thermal radiation, Aboeldahab and Gendy [14] explored magneto hydrodynamic convective gases moving across a moderately flat channel having changeable thermal parameters over large thermal resistance that computationally use the shooting technique. Rotating and intermittent heat differences' influence upon natural convection flow were researched by Friedrich and Rudraiah [15]. A hydromagnetic fluid's movement, including heat transmission over a stretched sheet under significant thermogenesis conditions, was described by Mostafa and Shima [16]. Recently,

Regarding the broader concepts of heat with mass transfer transmission, Kumar and Kansal [17] spoke about wave function, including the basic result. Bourantas and Loukopoulos [18] subsequently developed an illustration containing the hydromagnetic nanoliquids' convection circulation. Researchers looked into the fact that these microrotations generally reduce the amount of temperature that is transmitted from the heating surface, so their findings shouldn't have been disregarded. According to Patrulescu et al. [19], raising the weight percentage of Cu nanostructures enhances their heat capacity, which causes a heat transfer surface to expand through a combination of convection and radiation across a cone's horizontal circular shape. The structural uniqueness of microscopic creation of a ferromagnetic nanofluid having efficient heat capacity through a stretched surface, in addition to the mathematical model containing a micropolar movement across a circular cylinder, were covered by Anwar and Guram [20]. Umavathi et al. [21] have documented the effect of hydrostatic pressure inside a variable viscosity flow with micropolar across a cylindrical. The result demonstrates that the decrease characteristic for heat transfer is shown by the influence of the buoyant (combined convection) factor. The effects of thermal cubic expansion due to hydrostatic pressure, which produces a greater thickness of liquid, make the heat flow drop lower. Alharbi et al. [22] say that an unstable oscillation and a stretched porosity in a magneto hydrodynamics radiated Eyring–Powell fluid create energy. Venkatadri et al. [23] hypothesised convective Magneto hydrodynamic nanoparticle streams through a saturated porous media involving phase separation. Circulation among two simultaneous discs with an indefinite radius can be observed in the research of Bhat and Katagi [24], making it intriguing to take into account that the disc is both permeability and impenetrability.

Moreover, somewhere near permeable interface, this velocities displacement field will be used. B. Saidulu [25] Assessment of coupled mass along with energy transport during porous medium with electrochemical for magnetohydrodynamic micropolar circulation over a stretched surface. In the context of a Halls, radiative, Vorticity, as well as Viscous dissipation influences, Shateyi et al [26] investigation looked at how a magnetism affected energy including mass transport through mhd flow over flat sheet. Huang et al. [27] have explored that continuous fluid flows over an angled stretched sheet in the existence of chemical change with heat transfer and dispersion influences. Bataller [28] conducted an experimental study on the characteristics of velocity and molecular diffusion for various viscosity flow regimes affected by a porous stretched shrinking surface. This issue of properly mature convective heat and mass transport of a hydromagnetic fluid through a horizontal path has been examined by Sami Bataineh et al. [29] by a homotopy analytical approach. Bachok et al. [30] demonstrated the impact of thermal transport across an ill-defined stretched surface inside a micropolar. Recently, Aurangzaib et al. [31] looked at how heat and matter move down a segment in a nanofluid flow in a way that is not smooth. Ariman et al. [32] provided an outstanding overview of hydromagnetic fluids with related implications. Aman et al. [33] had spoken of temperature, motion, and frequency shear force for proportional boundary conditions inside an elastic material utilising computational LT. The impact of radiant heat upon properly advanced magneto hydrodynamic micropolar circulation of fluids via twin infinitely identical porosity longitudinal surfaces was examined by Prakash and Muthamilselvan [34].

When thinking about different medical problems, the relationship between temperature and heat exchange is a very important subject. According to Ziabakhsh et al. [35], hydromagnetic flow

patterns and heat production are possible. Toki [36] looked into the spontaneous free convection of an unstable magnetohydrodynamic fluid and found accurate results about how it flows. Elgazery [37] examined how heat-dependent viscousness along with heat transfer affected the impact of chemical reactions in magnetohydrodynamics. An immiscible, unstable hydromagnetic circulation over a perpendicular porous material was numerically solved by Islam et al. [38]. In his study of the flow pattern of a viscoelastic incompressible across porosity barriers, Berman [39] took into account the fluid's viscosity. A micropolar fluid having consequent effects on temperature flow separation over a stretched surface by Ishak[40].

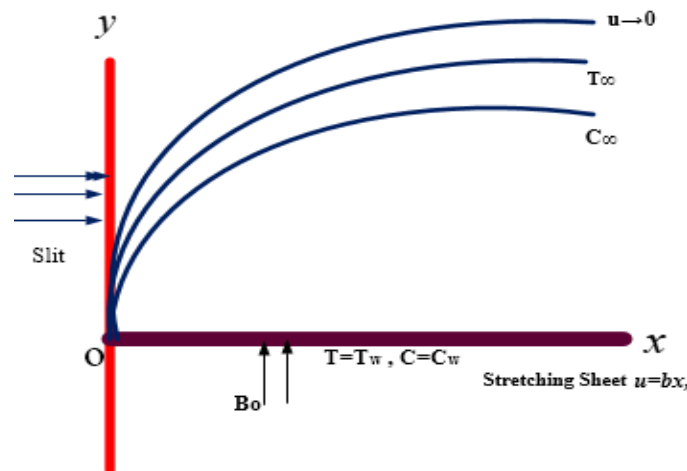
Our research aims to find a way to address the issue of heat and mass transfer in a steady mixed convection flow of an incompressible micropolar fluid over a stretched surface under influence based on thermal radiation and chemical reaction. Those expressions describing the modified fluid properties appear to be nonlinear and are unable to be resolved computationally. To deal with the issue numerically, we made use of MATLAB's

built-in solver. Researchers have investigated how important flow factors are to flow distribution functions. Both visual and graphical presentations of the results were made

MATHEMATICAL ANALYSIS

We consider a stretched plate guiding a continuously 2D homogeneous circulation of an incompressible micropolar at temperature T_∞ along a determined heat flux across the surface. The flow is thought to be in the x-axis, which therefore accelerates the sheet along its leading path, as well as the y-axis, which is thought to be opposed to it. A standard relationship between the flow direction and the y-axis is constructed, and this connection really does have a variable magnetic field. No connectivity to an outside electric field exists. Also, because of the lower Reynolds number, there is little interaction between the magnetic field generated by the fluid flow and the magnetic field that immediately accompanies it. These assumptions lead to the flow geometry of the issue, which can be seen in Figure 1, and the boundary layer equations

that explain steady flow over a stretching surface, which are as shown in;



1.Flow geometry

Continuity: $\frac{\partial u}{\partial x} + \frac{\partial v}{\partial y} = 0$... (1)

Momentum: $\frac{\partial u}{\partial x} + v \frac{\partial u}{\partial y} = \left(\nu + \frac{k}{\rho} \right) \frac{\partial^2 u}{\partial y^2} + \frac{k}{\rho} \frac{\partial N^*}{\partial y} - \frac{\sigma B_0^2}{\rho} u + g\beta_T(T - T_\infty) + g\beta_C(C - C_\infty)$..(2)



Angular momentum: $u \frac{\partial N^*}{\partial x} + v \frac{\partial N^*}{\partial y} = \frac{\gamma^*}{j\rho} \frac{\partial^2 N^*}{\partial y^2} - \frac{k}{j\rho} \left(2N^* + \frac{\partial u}{\partial y} \right)$... (3)

Energy: $u \frac{\partial T}{\partial x} + v \frac{\partial T}{\partial y} = \frac{k}{\rho C_p} \frac{\partial^2 T}{\partial y^2} + \frac{16\sigma^* T_\infty^3}{3k^* \rho C_p} \frac{\partial^2 T}{\partial y^2}$... (4)

Concentration: $u \frac{\partial C}{\partial x} + v \frac{\partial C}{\partial y} = D \frac{\partial^2 C}{\partial y^2} - k_1(C - C_\infty)$... (5)

The appropriate substantial border conditions

$$\left. \begin{aligned} u = u_w = bx, v = 0, N^* = -m_0 \frac{\partial u}{\partial y}, T = T_w, C = c_w \text{ at } y = 0 \\ u \rightarrow 0, N^* \rightarrow 0, T \rightarrow 0, C \rightarrow 0 \text{ as } y \rightarrow \infty \end{aligned} \right\} \dots (6)$$

The right-hand side of Eqn. (4) indicates components for viscous dissipation and the Ohmic heating effect. Here $\gamma^* = \left(\mu + \frac{k}{2} \right) j$ and $j = \frac{v}{c}$.

The heat flux flow $q_r = -\frac{4\sigma^*}{3\alpha^*} \frac{\partial T^4}{\partial y}$... (7)

We assume that the flow's internal temperature gradient is insignificant adequate for T^4 to be expressed as a linear average of the temperatures. The Taylor series expansion gives roughly T_∞ when T^4 is increased.

$$T^4 \approx 4T_\infty^3 T - 3T_\infty^3 \dots (8)$$

Hence,

$$\frac{\partial q_r}{\partial y} = -\frac{16\sigma^* T_\infty^3}{3\alpha^*} \frac{\partial^2 T}{\partial y^2} \dots (9)$$

We use the similarity transformations and dimensional parameters listed further to transform Eqs. (2)– (5) along with Eqs. (7 and 9) into a scheme containing ordinary differential equations.

$$\left. \begin{aligned} \zeta = \left(\sqrt{\frac{b}{v}} \right) y, u = cx f'(\zeta), v = -\sqrt{cv} f(\zeta) \\ N^* = \sqrt{\frac{b^3}{v}} x g(\zeta), \theta(\zeta) = \frac{T - T_\infty}{T_w - T_\infty}, \phi(\zeta) = \frac{C - C_\infty}{C_w - C_\infty} \end{aligned} \right\} \dots (10)$$

Eqn (1) is indeed valid with in circumstances of eqs(1) - (5). These additional solutions within that situation were condensed to a preceding.

$$(1 + K)f''' + ff'' - (f')^2 + Kg' - M^2 f' + \lambda(\theta + N\phi) = 0 \dots (11)$$

$$\left(1 + \frac{K}{2} \right) g'' + fg' - gf' - K(2g + f'') = 0 \dots (12)$$

$$(1 + N_R)\theta'' + Prf\theta' = 0 \dots (13)$$

$$\phi'' + scf\phi' - Sc\gamma\phi = 0 \dots (14)$$

The modified border circumstances include

$$\left. \begin{aligned} f(\zeta) = 0, f'(\zeta) = 1, g(\zeta) = -m_0 f''(\zeta), \theta(\zeta) = 1, \phi(\zeta) = 1 \text{ at } \zeta = 0 \\ f'(\zeta) = 0, g(\zeta) = 0, \theta(\zeta) = 0, \phi(\zeta) = 0 \text{ as } \zeta \rightarrow \infty \end{aligned} \right\} \dots (15)$$

Thus, these dimensional less parameters become, while prime represents the derivatives with respect to ζ .

$$\left. \begin{aligned} K = \frac{k}{\mu}, M^2 = \frac{\sigma B_0^2}{\rho b}, Pr = \frac{\mu c_p}{k_f}, N_R = \frac{16\sigma^* T_\infty^3}{3k^* k_1}, Sc = \frac{v}{D} \\ \gamma = \frac{K_1}{b}, \lambda = \frac{Gr_x}{Re_x^2}, Gr_x = \frac{g\beta(T_w - T_\infty)x^3/u^2}{u_w^2 x^2/u^2}, N = \frac{\beta_C(C_w - C_\infty)}{\beta_T(T_w - T_\infty)} \\ C_{fx} = \frac{[(\mu + \kappa) \frac{\partial u}{\partial y} + \kappa N]_{y=0}}{\rho u_w^2}, N_u = \frac{-x \left(\frac{\partial T}{\partial y} \right)_{y=0}}{(T_w - T_\infty)}, S_h = \frac{-x \left(\frac{\partial C}{\partial y} \right)_{y=0}}{(C_w - C_\infty)} \end{aligned} \right\} \dots (16)$$

would have that system result upon applying (10).

$$Re_x^{\frac{1}{2}} C_{fx} = [1 + (1 - m_0 K) f''(0)],$$

$$N_u Re_x^{\frac{-1}{2}} = -\theta'(0), S_h Re_x^{\frac{-1}{2}} = -\phi'(0).$$



Where $Re_x = \frac{\alpha x^2}{\nu}$ is the local Reynolds number.

METHOD OF SOLUTION

An approximation can be obtained by converting the joint initiative of nonlinear ordinary differential equations (11) through (14) and the border conditions (15) into an initial value issue. We built $y_1 = f, y_2 = f', y_3 = f'', y_4 = g, y_5 = g', y_6 = \theta, y_7 = \theta', y_8 = \phi, y_9 = \phi'$ then the nonlinear ODEs are transformed into the following form

$$y'_3 = -(y_1 * y_3 - y_2 * y_2 - (M * M * y_2) + (K * y_5) + (\lambda * (y_6 + N * y_8)))/(1 + K)$$

$$y'_5 = -((y_1 * y_5) - (y_2 * y_4) - (K * (2 * y_4 + y_3)))/(1 + K/2)$$

$$y'_7 = -(Pr * y_1 * y_7)/(1 + N_R)$$

$$y'_9 = -(sc(y_1 * y_9) - Sc * \gamma * y_8)$$

The boundary constraints are

$$y_1(0) = 0, y_2(0) = 1, y_4(0) = -m_0 y_3(0), y_6(0) = 1, y_8(0) = 1$$

$$y_2(\infty) = 0, y_4(\infty) = 0, y_6(\infty) = 0, y_8(\infty) = 0$$

The resulting ODE can then be integrated using MATLAB's built-in solver approach. The foregoing procedure is repeated till the results reach sufficient precise degree 10^{-6} . The built-in solver technique in MATLAB can be used to integrate the following ODE. Such a process is repeated till the results match the desired level of accuracy, like, 10^{-6} .

RESULTS AND DISCUSSION

Using the built-in MATLAB programme, these estimated functions of velocity, microrotation,

temperature, and concentration are all represented graphically as displayed in figs. 2–21. Within those analyses, the Prandtl number (Pr) is kept stable only by the value of 0.7 used in prior studies, and the effects of parameters for the magnetic field (M), buoyancy ratio (N), material (K), radiation (Nr), local buoyancy parameter λ and the Schmidt number (Sc), chemical reaction parameter (γ) is investigated

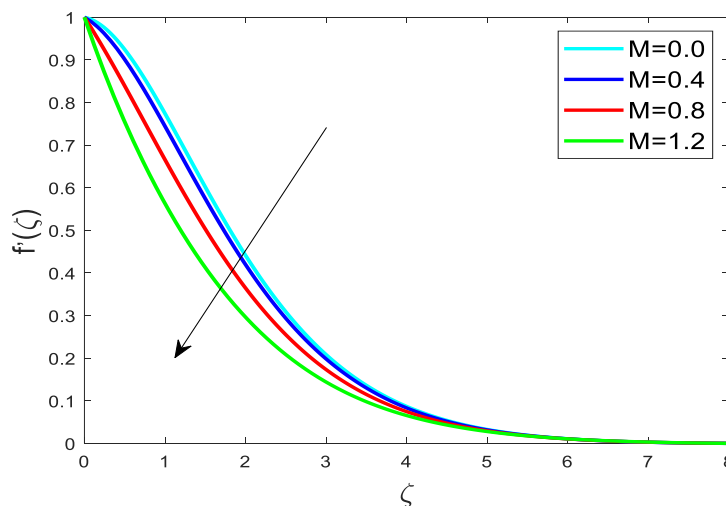


Fig.2: M v/s velocity. $Pr=0.7, N=1, Sc=0.5, Nr=0.2, \lambda=0.5, K=1.0, m_0=0.5$.

Figure 2 illustrates how the velocity function depends on the magnetic parameter (M). This demonstrates that velocity decreases as M rises. This shows that a larger magnetic field can cause a fluid to flow more slowly. But, when M increases, the flow border surface's depth falls. This is due to the fact that when a magnetic field is applied to a fluid that conducts electricity, the fluid's velocity slows down.



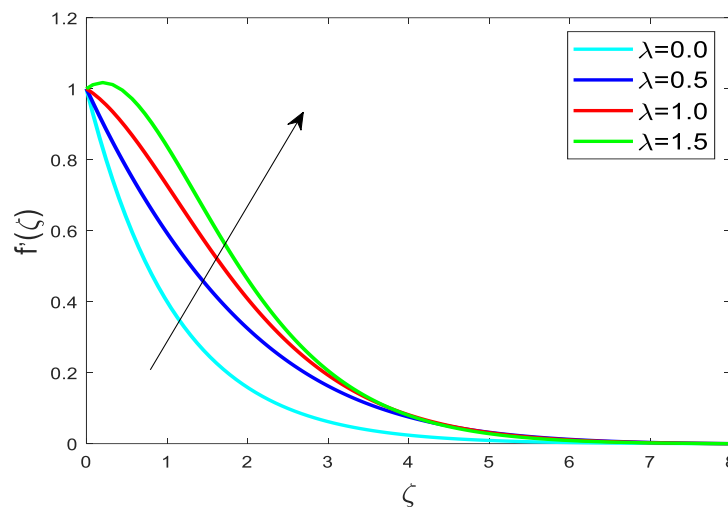


Fig3: λ v/s velocity. $Pr=0.7, N=1, Sc=0.5, Nr =0.2, M=0.5, K=1.0, m_0=0.5$.

Fig3 depicts the influence of a buoyant force value upon this velocity distribution. The velocity profile was found to rise down as the buoyant force value rises .

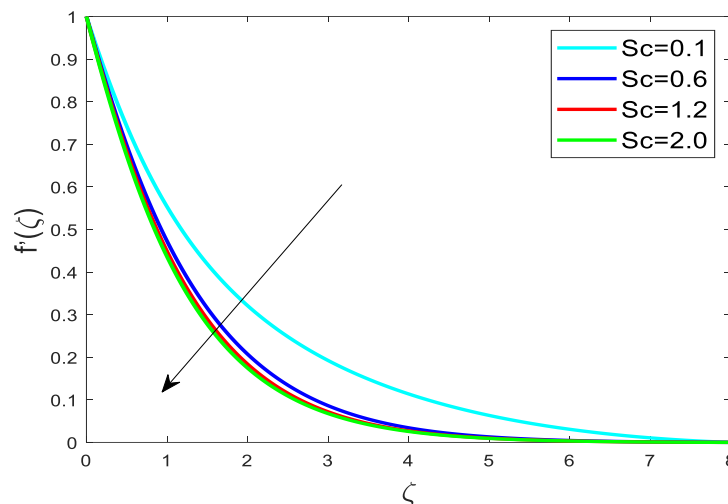


Fig4: Sc v/s velocity. $Pr=0.7, N=1, \gamma=1.0, Nr =0.2, \lambda=0.5, M =0.5, K=1.0, m_0=0.5$.

The velocity profile diminishes even as Schmidt's value rises. It is discovered when increasing its Schmidt value greatly slows the fluid's flow, i.e., its velocity drops. When Sc increases, the chemically determined diffusion coefficient of a component decreases, including the concentration border layer, which gets narrower than the viscosity border layer.

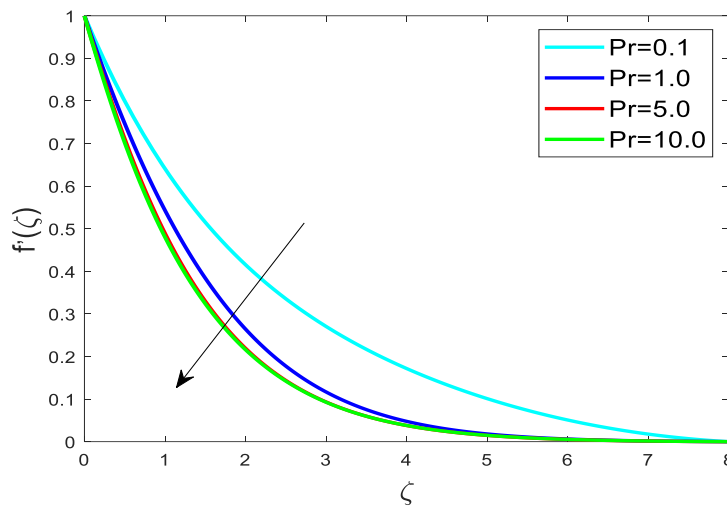


Fig5:Pr v/s Velocity. $Sc = 0.5, N=1, \gamma=1.0, Nr =0.2, \lambda=0.5, M =0.5, K=1.0, m_0=0.5$.
 Figure 5 depicts the influence of a Prandtl value upon this velocity distribution. The velocity profile was found to falls down as the Prandtl values rises.

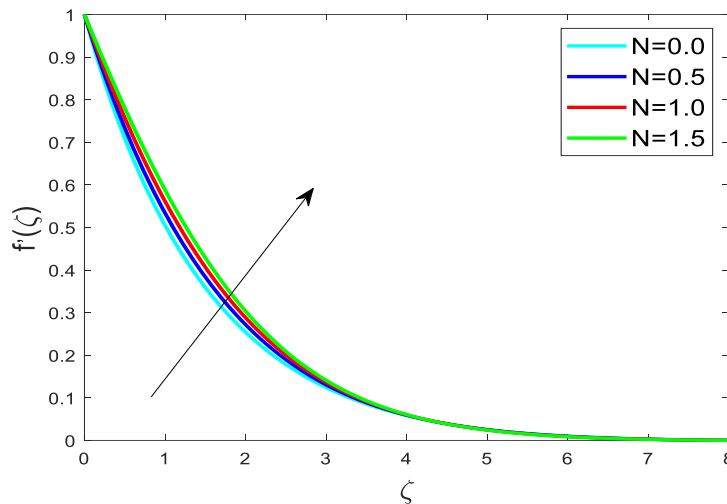


Fig.6: N v/s Velocity, $Sc=0.5, M =0.5, m_0=0.5, Pr=0.7, K=1.0, \gamma=1.0, Nr=0.2, \lambda=0.5$.
 Fig 6 examines the distribution of velocity in a current system and shows the variation in the buoyancy ratio N.It is discovered that when N increases ,the curvature of a velocity distribution increases.

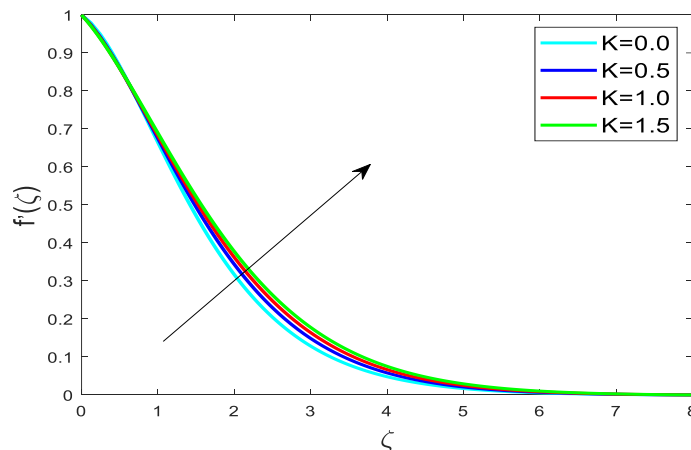
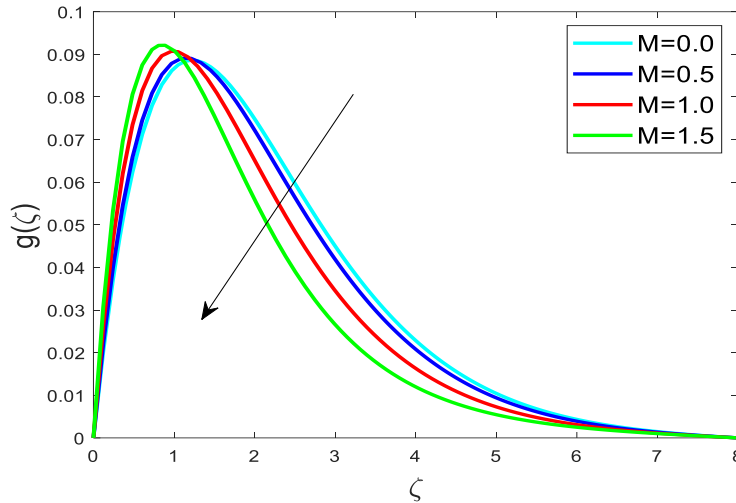


Fig.7: K v/s Velocity. $Pr=0.7, M =0.5, Nr=0.2, \lambda=0.5, N=1.0, \gamma=1.0, m_0=0.5, Sc=0.5$.

Figure 7 depicts the ratio between velocity and the material parameter K. The graphic unequivocally demonstrates that as K is increased, velocity increases. When the micro concentration of a substance rises, so does its material parameter. As a simple consequence, the micro concentration changes the flow field. It shows that such a material element increases the depth of a flow separation.



4698

Fig.8: M v/s Microrotation profile. $\gamma=1.0, Nr=0.2, \lambda=0.5, K=1.0, Sc=0.5, m_0=0.0, Pr=0.7$.

When the magnetic parameter M is changed, the microrotation distribution changes, as seen in Figure 8. It is demonstrated that the enlarged quantities of M cause comparable microrotation, showing that it originally grows, then begins to decrease when $\zeta = 1$. The dynamic viscosity declines with escalating values of M.

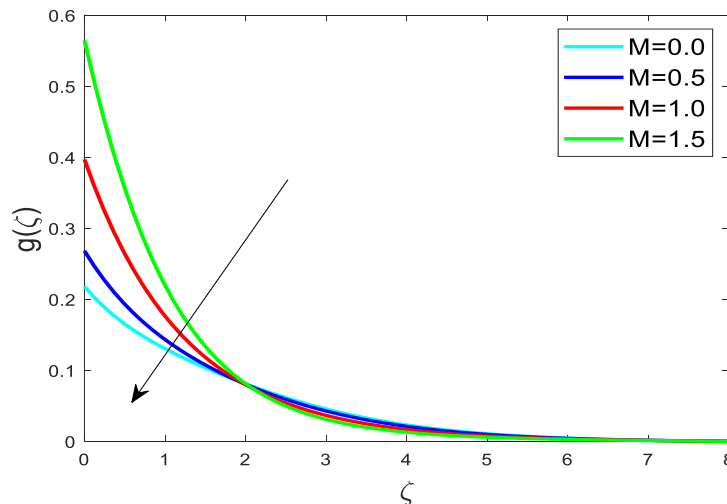


Fig9: M v/s Microrotation. $Pr=0.7, Sc=0.5, \gamma=1.0, Nr=0.2, \lambda=0.5, K=1.0, m_0=0.5$.

The varying microrotation distribution once the magnetic number M is changed is shown in Figure 9. It is demonstrated that increased quantities of M induce microrotation to increase in a comparable way.



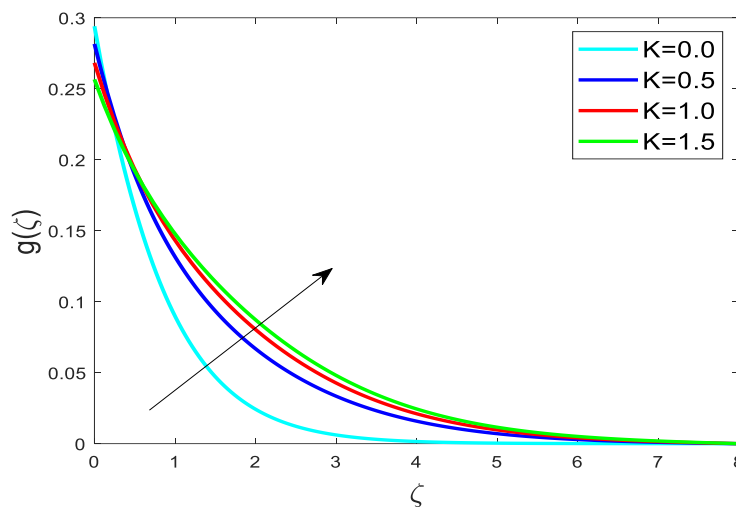


Fig10: K v/s Microrotation. $M = 0.5, \lambda = 0.5, Pr = 0.7, \gamma = 1.0, Nr = 0.2, m_0 = 0.5, Sc = 0.5$.
 When material factor K is changed, its microrotation distribution changes, as shown in Figure 10. It is demonstrated that increased levels of K cause comparable microrotation, showing that it originally falls down, then begins to rise when $\zeta = 0.5$.

4699

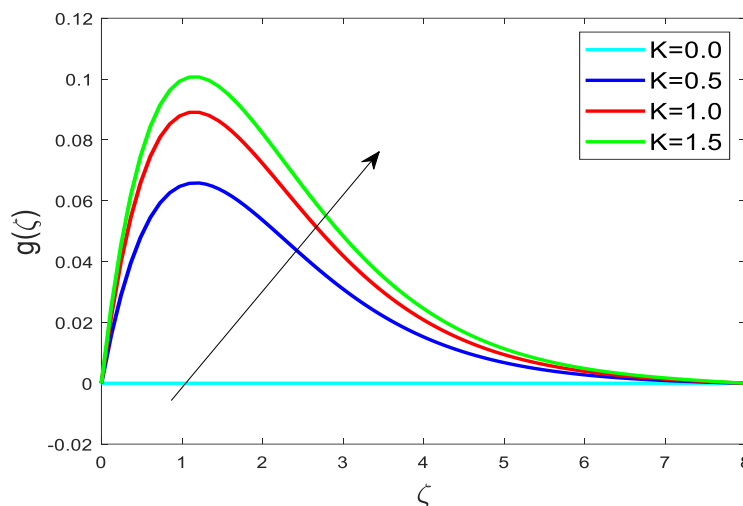


Fig.11: K v/s Microrotation, $M = 0.5, \lambda = 0.5, Pr = 0.7, \gamma = 1.0, Nr = 0.2, m_0 = 0.5, Sc = 0.5$.

Figure 11 depicts the influence of a material parameter value upon this microrotation distribution. The microrotation profile was found to rise as material parameter values rises.



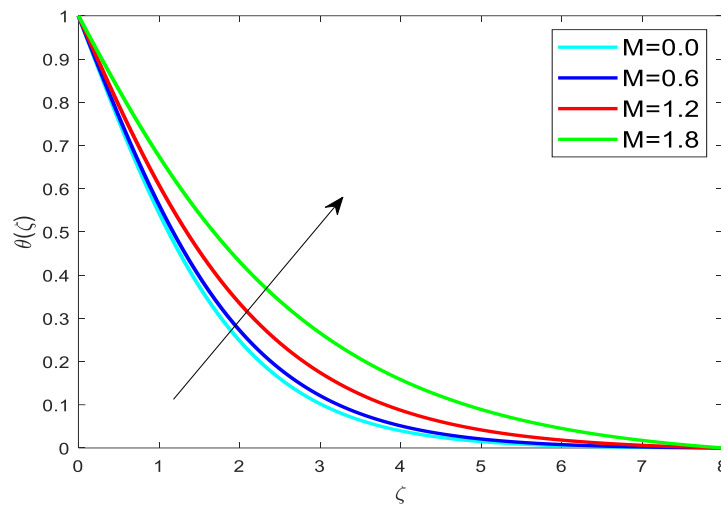
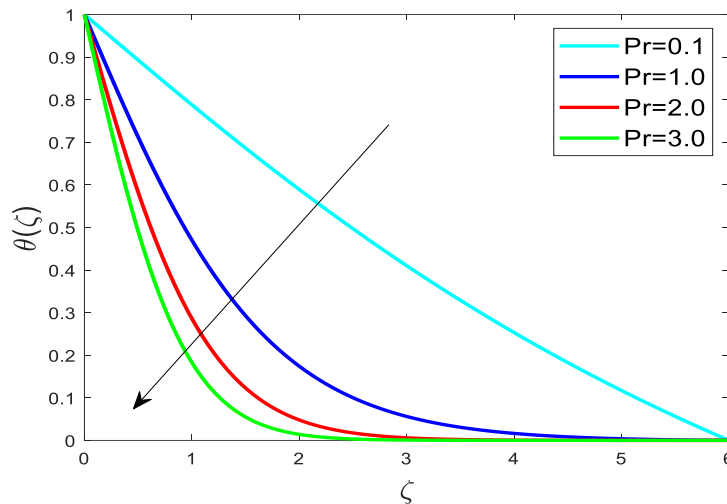


Fig.12: M v/s Temperature. $Pr=0.7$, $Sc=0.5$, $N=1$, $Nr=0.2$, $\lambda=0.5$, $K=1.0$, $m_0=0.5$.
 Figure 12 depicts visually the joint connection among temperature and there is magnetic field strength. The graph indicates everything as M increases, temperature rises as impact.



4700

Fig.13: Pr v/s Temperature. $Sc=0.5$, $\gamma=1.0$, $N=1.0$, $Nr=0.2$, $\lambda=0.5$, $M=0.5$, $K=1.0$, $m_0=0.5$.
 Figure 13 illustrates how the Prandtl number affects the temperature distribution. Increased Prandtl numbers the fluid's temperature decreases as a result of the above.

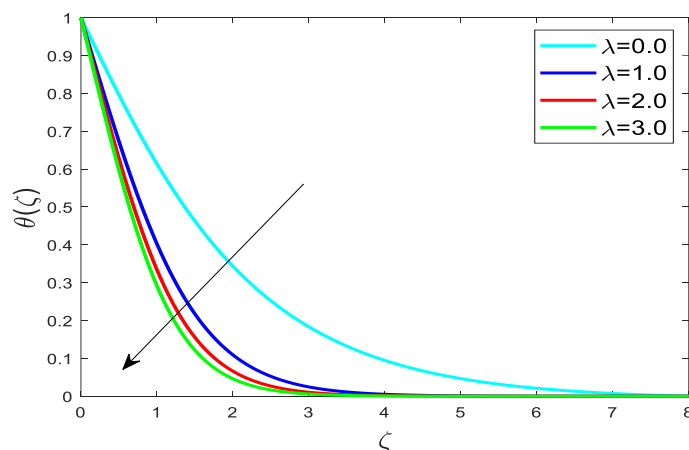


Fig.14: λ v/s Temperature profile. $Nr=0.2$, $Pr=0.7$, $N=1.0$, $K=1.0$, $m_0=0.5$, $Sc=0.5$, $M=0.5$.



Fig 14 Increased buoyance numbersthe fluid's temperature decreases as a result of the above.

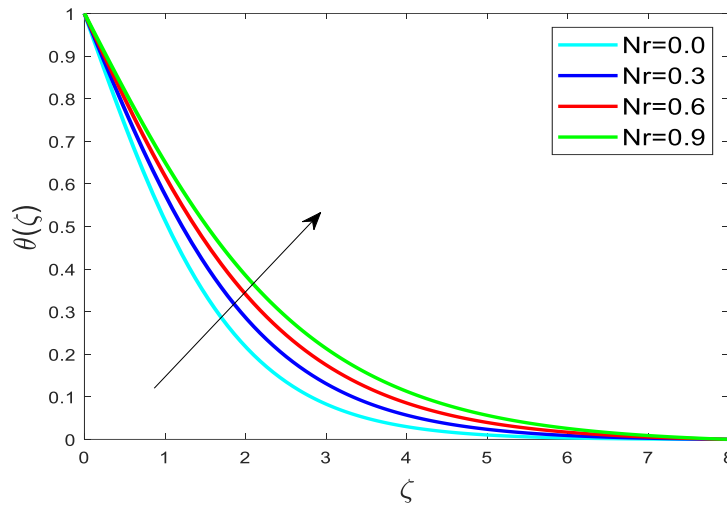


Fig.15: Nr v/s Temperature profile, $N=1.0, \lambda=0.5, M=0.5, K=1.0, m_0=0.5, Pr=0.7, Sc=0.5, \gamma=1.0$.
 Figure 15 depicts the effect of a radiation value of Nr. The temperature of the fluid rises because increased levels of the radiation value of Nr.

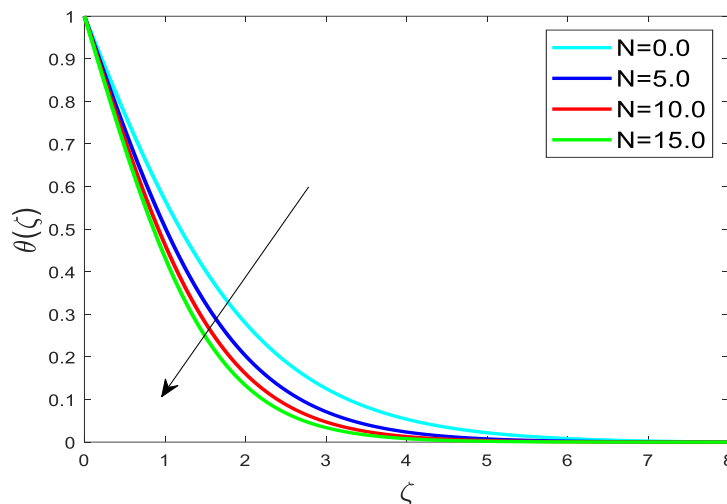


Fig.16: N v/s Temperature profile. $Pr=0.7, Sc=0.5, Nr=0.2, M=0.5, K=1.0, \gamma=1.0, \lambda=0.5, m_0=0.5$.
 Figure 16 shows how the temperature distribution adjusts to different quantities of the buoyancy ratio factor N. When N increases, the temperature decreases.

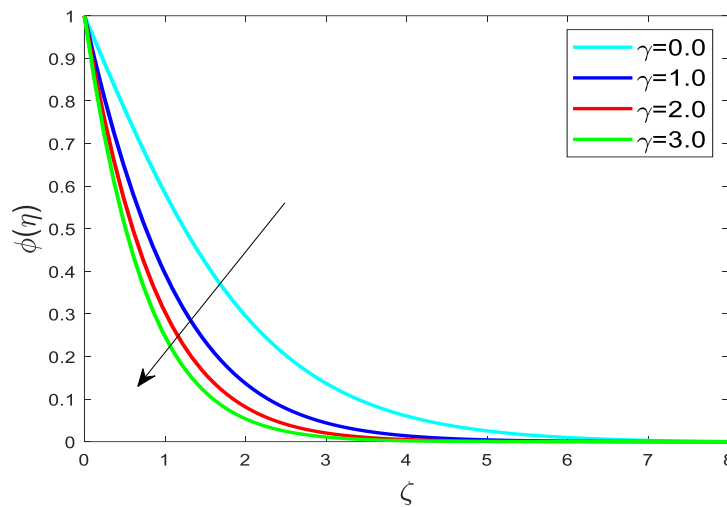


Fig.17: γ v/s Concentration. $N=1,0, Sc=0.5, Nr=0.2, M =0.5, K=1.0, \lambda=0.5m_0=0.5$.
 Fig. 17 illustrates the fluid concentration distribution drops as the quantity characterising the chemical reaction rises.

4702

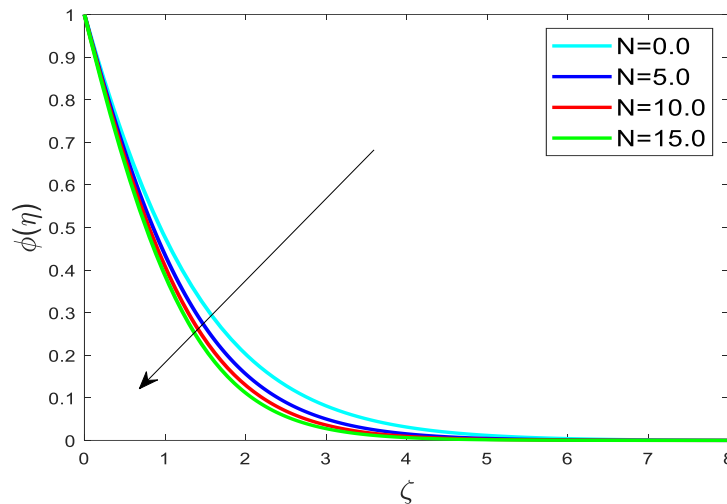


Fig.18: N v/s Concentration. $Pr=0.7, Sc=0.5, Nr=0.2, M =0.5, K=1.0, \gamma=1.0, \lambda=0.5m_0=0.5$.
 Figure 18 shows how the Concentration distribution adjusts to different quantities of the buoyancy ratio factor N . When N increases, Concentration decreases.

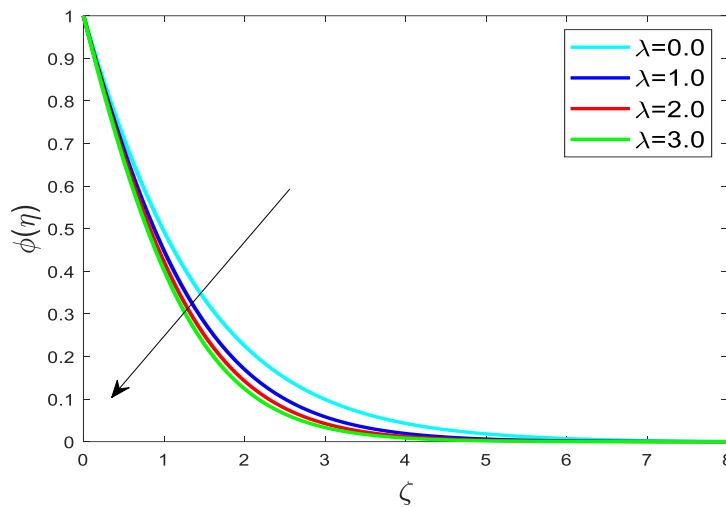


Fig.19: λ v/s Concentration. $Pr=0.7, Sc=0.5, Nr=0.2, M=0.5, K=1.0, N=1, m_0=0.5$.

Figure 19 shows how the Concentration distribution adjusts to different quantities of the buoyancy factor λ . When λ increases, Concentration decreases.

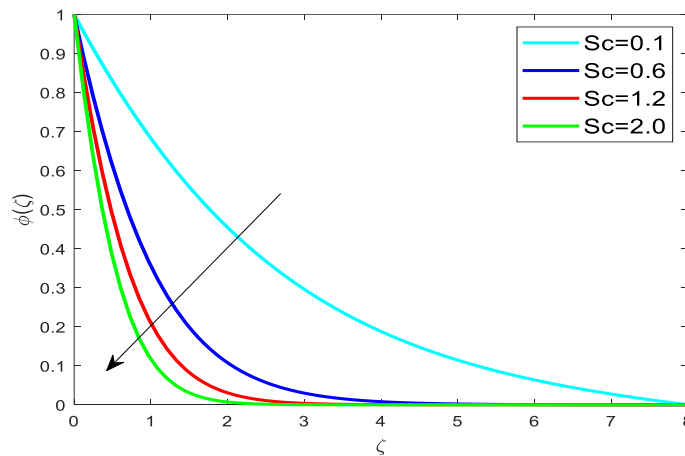


Fig.20: Sc v/s Concentration. $Pr=7, Nr=0.2, M=0.5, K=1.0, \gamma=1.0, N=1.0, \lambda=0.5, m_0=0.5$.
 Figure 20 depicts with an increase in Schmidt number Sc , concentration is shown to decline.

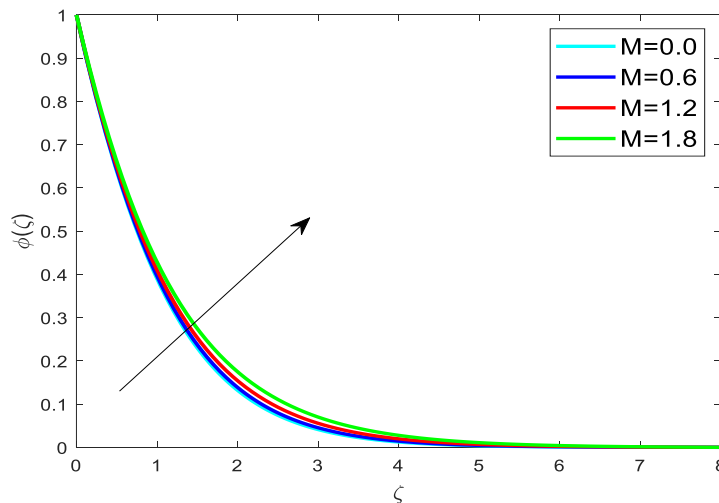


Fig.21: M v/s Concentration. $Pr=0.7, S_c=0.5, N_R=0.2, N=1, K=1.0, \lambda=0.5, m_0=0.5$.



Figure 21 displays a concentration graph versus magnetic field level. Fundamentally, it makes sense that concentration increases as M increases because a greater M restricts molecule migration for repositioning. As a result, the parameter M can be used to control the temperature and the velocity. Table1 compares $-\theta'(0)$ for a variety of Nr, Pr, K quantities given at $m_0=0.5$ throughout

the absence, like several additional influences. Skin friction coefficient quantities are shown in Table 2 for variations in N, λ and K and constant quantities of $Pr = 0.7, Sc=0.5, M = 1,$ and $\gamma = 1$. Table 3 shows a certain Sharewood number increasing as parameters M, Sc, K have been increased, while $m_0=0.5$. and are kept at $N= 0.0$ and $\lambda = 0.0$, respectively.

Table-1: Comparison of $-\theta'(0)$ for various values of Nr, Pr, K with $m_0=0.5$.

Nr	K	Pr	M	Previous study Ishak, A [40]	Present Study $-\theta'(0)$
1.0	1.0	1.0	0.0	0.3893	0.390384
	2.0			0.4115	0.411954
2.0	0.0			0.2588	0.268852
	1.0			0.2895	0.295161
	2.0			0.3099	0.313376

4704

Table-2: Numerical values of Skin friction co-efficient $C_{f_x} Re_x^{\frac{1}{2}}$ for variation in N, K, λ with $Sc=0.5, \gamma=1, M=1 \& Pr=0.7$.

N	λ	K	$C_{f_x} Re_x^{\frac{1}{2}}$ at $m=0.0$	$C_{f_x} Re_x^{\frac{1}{2}}$ at $m=0.5$
0.0	0.5	0.7	-1.427319	-1.275530
1.0			-1.189017	-1.061684
2.0			-0.955682	-0.852721
3.0			-0.726750	-0.648043
1.0	0.0	1.0	-1.942220	-1.706491
	0.2		-1.671993	-1.465377
	0.5		-1.293542	-1.130946
	1.0		-0.706710	-0.616276
1.0	0.5	0.0	-0.887530	-0.887535
		0.5	-1.113031	-1.013948



		1.0	-1.293542	-1.130946
		1.5	-1.449594	-1.240979

Table-3: Numerical solution of $-\phi'(0)$ for various values of M, Sc, K with $m_0=0.5$.

Sc	γ	K	M	N	λ	$-\phi'(0)$
0.5	1.0	1.0	0.5	0.0	0.0	0.820814
1.2						1.299935
2.0						1.696163
0.5	1.0	1.0	0.5			0.820814
0.5	2.0					1.088921
0.5	3.0					1.301076
0.7	1.0	1.0	0.5	0.0	0.0	0.979970
0.7		2.0				0.987018
0.7		4.0				0.996171
0.7	1.0	1.0	0.0			0.985505
			0.5			0.979970
			1.5			0.954290
0.5	1.0	1.0	1.0	1.0	0.5	0.828554
				2.0		0.834523
				3.0		0.840207
				1.0	0.0	0.80988
					1.0	0.843129
					2.0	0.866707

4705

CONCLUSIONS

Throughout the context of the present work, we have looked upon heat and mass transfer



on steady mixed convection flow of incompressible a micropolar fluid through a stretched sheet in the presence of the thermal radiation. The regulating flow problem might be simplified using similarity transformations. The Runge-Kutta Technique and the bvp4c solver are coupled in an attempt to quantitatively analyse the resulting nonlinear ODEs. The conclusions that follow were inferred from current research.

- Whenever the magnetic factors have been raised, the velocity drops; however, if the material factors and buoyancy ratio parameter are raised, the velocity rises.
- Microrotation grows when M and the surface condition parameter rise, but it reduces when K rises.
- The M and Nr factors can be changed to raise the temperatures. Hence, a higher temperature may be reached simply by modifying certain variables.
- Concentration increases as M increases, although this decreases when the buoyancy factor, buoyancy ratio factor, and Schmidt number increase.

REFERNACE:

[1] J. Peddieson and R. P. Mcnitt, Boundary layer theory for a micropolar fluid, *Recent Advances in Engineering Science* 5 (1970), 405–426.
[2] G. Ahmadi, Self-similar solution of incompressible micropolar boundary layer flow over a semi infinite plate, *International Journal of Engineering Science* 14 (1976), no. 7, 639–646.
[3] Y. J. Kim, “Unsteady MHD convection flow of polar fluids past a vertical moving porous plate in a porous medium,” *International Journal of Heat and Mass Transfer*, vol. 44, no. 15, pp. 2791–2799, 2001.
[4] E. M. Abo-Eldahab and A. F. Ghonaim, “Radiation effect on heat transfer of a micropolar fluid through a porous medium,” *Applied Mathematics and Computation*, vol. 169, no. 1, pp. 500–510, 2005.

[5] R. Berker, *Integration des Equations du Movement d'un Fluid Visquent Incompressible*, Hand Book of Fluid Dynamics, vol. 3, Springer, Berlin, Germany, 1963.

[6] J. Coirier, “Rotations non coaxials d'un disque et d'un fluide a l'infini,” *Journal de Mecanique*, vol. 11, pp. 317–340, 1972.

[7] S. K. Jena and M. N. Mathur, “Similarity solutions for laminar free convection flow of a thermomicropolar fluid past a nonisothermal vertical flat plate,” *International Journal of Engineering Science*, vol. 19, no. 11, pp. 1431–1439, 1981.

[8] K. B. Pavlov, “Magnetohydrodynamic flow of an incompressible viscous fluid caused by deformation of a surface,” *Magnitnaya Gidrodinamika*, vol. 4, pp. 146–147, 1974.

[9] J. D. Lee and A. C. Eringen, “Wave propagation in nematic liquid crystals,” *The Journal of Chemical Physics*, vol. 54, no. 12, pp. 5027–5034, 1971.

[10] N. G. Kafoussias and E. W. Williams, “Thermal-diffusion and diffusion-thermo effects on mixed free forced convective and mass transfer boundary layer flow with temperature dependent viscosity,” *International Journal of Engineering Science*, vol. 33, no. 9, pp. 1369–1384, 1995.

[11] S. N. Gaikwad, M. S. Malashetty, and K. Rama Prasad, “An analytical study of linear and non-linear double diffusive convection with Soret and Dufour effects in couple stress fluid,” *International Journal of Non-Linear Mechanics*, vol. 42, no. 7, pp. 903–913, 2007.

[12] M. A. Hossain and H. S. Takhar, “Radiation effect on mixed convection along a vertical plate with uniform surface temperature,” *Heat and Mass Transfer*, vol. 31, no. 4, pp. 243–248, 1996.

[13] P. Ramamoorthy, “Heat transfer in hydromagnetics,” *The Quarterly Journal of Mechanics and Applied Mathematics*, vol. 18, pp. 31–40, 1965.

[14] E. M. Aboeldahab and M. S. El Gendy, “Radiation effect on MHD free-convective flow of a gas past a semi-infinite vertical

plate with variable thermophysical properties for high-temperature differences,” Canadian Journal of Physics, vol. 80, no. 12, pp. 1609–1619, 2002.

[15] R. Friedrich and N. Rudraiah, “Marangoni convection in a rotating fluid layer with non-uniform temperature gradient,” International Journal of Heat and Mass Transfer, vol. 27, no. 3, pp. 443–449, 1984.

[16] A. A. M. Mostafa and E. W. Shamaa, “MHD flow and heat transfer of a micropolar fluid over a stretching surface with heat generation (absorption) and slip velocity,” Journal of the Egyptian Mathematics Society, vol. 20, pp. 20–27, 2012.

[17] R. Kumar and T. Kansal, “Plane waves and fundamental solution in the generalized theories of thermoelastic diffusion,” International Journal of Applied Mathematics and Mechanics, vol. 8, pp. 1–20, 2012.

[18] Bourantas GC, Loukopoulos VC. Modeling the natural convective flow of micropolar nanofluids. Int J Heat Mass Transfer. 2014;68:35-41.

[19] Patrulescu FO, Grosan T, Pop I. Mixed convection boundary layer flow from a vertical truncated cone in a nanofluid. Int J Num Methods Heat Fluid Flow. 2014;24(5):1175-1190.

[20] Anwar M, Guram GS. Numerical solution of a micropolar flow between a rotating and a stationary Disc. Comput Maths with Appl 1980;6:235-245.

[21] Umavathi JC, Sheremet MA, Patil SL. Soret effects on the mixed convective flow using Robin boundary conditions. Heat Transfer-Asian Res. 2020; 49:154-179.

[22] Alharbi SO, Dawar A, Shah Z, et al. Entropy generation in MHD Eyring–Powell fluid flow over an unsteady oscillatory porous stretching surface under the impact of thermal radiation and heat source/sink. Appl Sci. 2018; 8:2588. <https://doi.org/10.3390/app8122588>.

[23] Venkatadri K, Abdul Gaffar S, Rajarajeswari P, Ramachandra Prasad V, Anwar Bég O, Hidayathulla Khan BM. Melting heat transfer analysis of electrically conducting nanofluid flow over an

exponentially shrinking/stretching porous sheet with radiative heat flux under a magnetic field. Heat Transfer. 2020;49(8):4281-4303.

[24] Bhat A, Katagi NN. Micropolar fluid flow between a non-porous disk and a porous disk with slip: Keller box solution. Ain Shams Eng J. 2020;11:149-159.

[25] Saidulu, B. " Role of Magnetic Field on Natural Convective Towards a Semi-Infinite Vertically Inclined Plate in Presence of Hall Current with Numerical Solutions: A Finite Difference Technique ", International Journal of Scientific and Innovative Mathematical Research, vol. 6, no. 2, p. 25-40, 2018., <http://dx.doi.org/10.20431/2347-3142.0602003>.

[26] Shateyi S, Motsa SS, Sibanda P. The effects of thermal radiation, hall currents, Soret and Dufour on MHD flow by mixed convection over a vertical surface in porous media. Math Prob Eng 2010;627475.

[27] Huang JS, Tsai R, Huang KH, Huang CH. Thermal-diffusion and diffusion thermo effects on natural convection along an inclined stretching surface in a porous medium with chemical reaction. Chem Eng Commun 2010;198:453–473.

[28] Bataller RC. Viscoelastic fluid flow and heat transfer over a stretching sheet under the effects of a non-uniform heat source, viscous dissipation and thermal radiation. Int J Heat Mass Transf 2007;50:3152.

[29] Sami Bataineh A, Noorani MSM, Hashim I. Solution of fully developed free convection of a micropolar fluid in a vertical channel by homotopy analysis method. Int J Numer Methods in Fluids 2009; 60:779.

[30] Bachok N, Ishak A, Nazar R. Flow and heat transfer over an unsteady stretching sheet in a micropolar fluid. Meccanica 2011; 46:935–942.

[31] Aurangzaib ARM, Mohammad NF, Shafie S. Unsteady MHD mixed convection flow of a micropolar fluid along an inclined stretching plate. Heat Transf Asian Res 2013; 42:89–99.

[32] T. Ariman, N. D. Sylvester, and M. A. Turk, “Applications of microcontinuum fluid mechanics,” International Journal of Engineering Science, vol. 12, no. 4, pp. 273–293, 1974.

[33] S. Aman, Q. Al-Mdallal, and I. Khan, "Heat transfer and second order slip effect on MHD flow of fractional Maxwell fluid in a porous medium," *Journal of King Saud University Science*, vol. 32, no. 1, pp. 450–458, 2020.

[34] D. Prakash and M. Muthtamilselvan, "Effect of radiation on transient MHD flow of micropolar fluid between porous vertical channel with boundary conditions of the third kind," *Ain Shams Engineering Journal*, vol. 5, no. 4, pp. 1277–1286, 2014.

[35] Z. Ziabakhsh, G. Domairry, and H. Bararnia, "Analytical solution of non-Newtonian micropolar fluid flow with uniform suction/blowing and heat generation," *Journal of the Taiwan Institute of Chemical Engineers*, vol. 40, no. 4, pp. 443–451, 2009.

[36] J. N. Tokis, "A class of exact solutions of the unsteady magnetohydrodynamic free-

convection flows," *Astrophysics and Space Science*, vol. 112, no. 2, pp. 413–422, 1985.

[37] N. S. Elgazery, "The effects of chemical reaction, Hall and ion-slip currents on MHD flow with temperature dependent viscosity and thermal diffusivity," *Communications in Nonlinear Science and Numerical Simulation*, vol. 14, no. 4, pp. 1267–1283, 2009.

[38] A. Islam, Md. H. A. Biswas, Md. R. Islam, and S. M. Mohiuddin, "MHD micropolar fluid flow through vertical porous medium," *Academic Research International*, vol. 1, no. 3, pp. 381–393, 2011.

[39] A. S. Berman, "Laminar flow in channels with porous walls," *Journal of Applied Physics*, vol. 24, pp. 1232–1235, 1953.

[40] Ishak, A. (2010). Thermal boundary layer flow over a stretching sheet in a micropolar fluid with radiation effect. *Meccanica*, 45, 367-373.